Supporting Information

Homologous NiO//Ni_2P Nanoarrays Grown on Nickel Foams: A Well Matched Electrode Pair with High Stability in Overall Water Splitting

Jinlong Zheng, Wei Zhou,* Tong Liu, Chengbo Wang, Shijie Liu and Lin Guo*

School of Chemistry and Environment, Beihang University, Beijing 100191, China

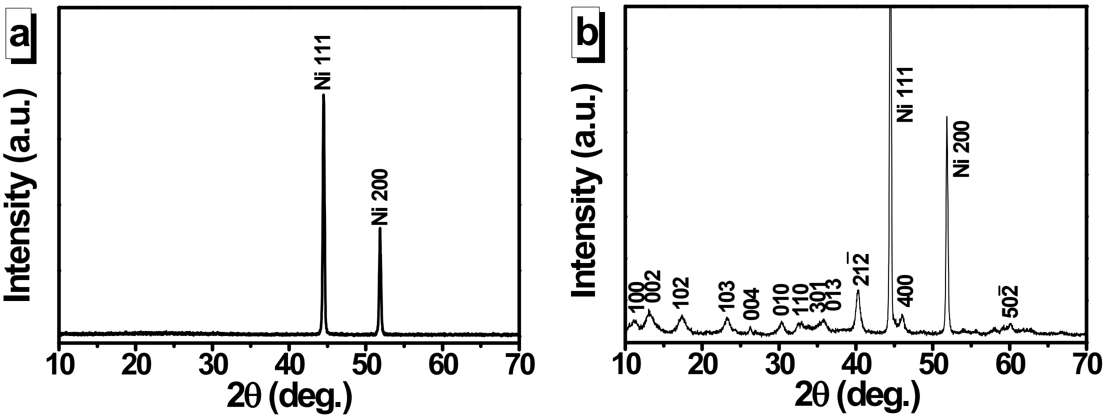

Fig. S1 (a) XRD pattern of Ni foam which can be indexed to cubic Ni (JCPDF No. 04-0850). (b) XRD pattern of the precursor. The peaks match well with the component of $Ni(SO_4)_{0.3}(OH)_{1.4}$ (JCPDS No. 41-1424).

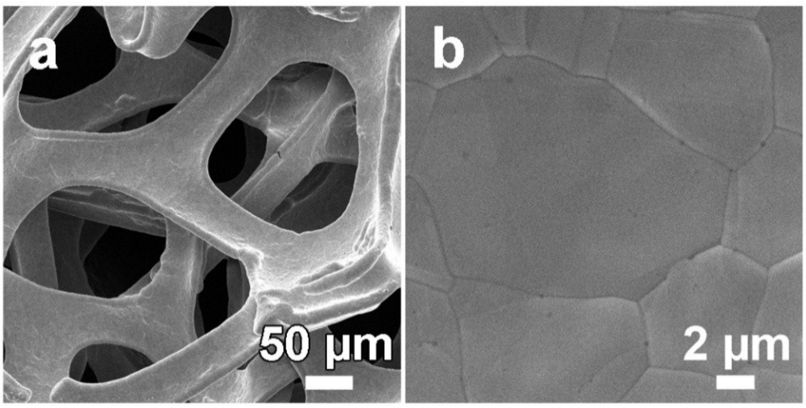

Fig. S2 (a, b) SEM images of Ni foam which was used as substrate to prepared the sample. The Ni foam has a clean surface after treatment.

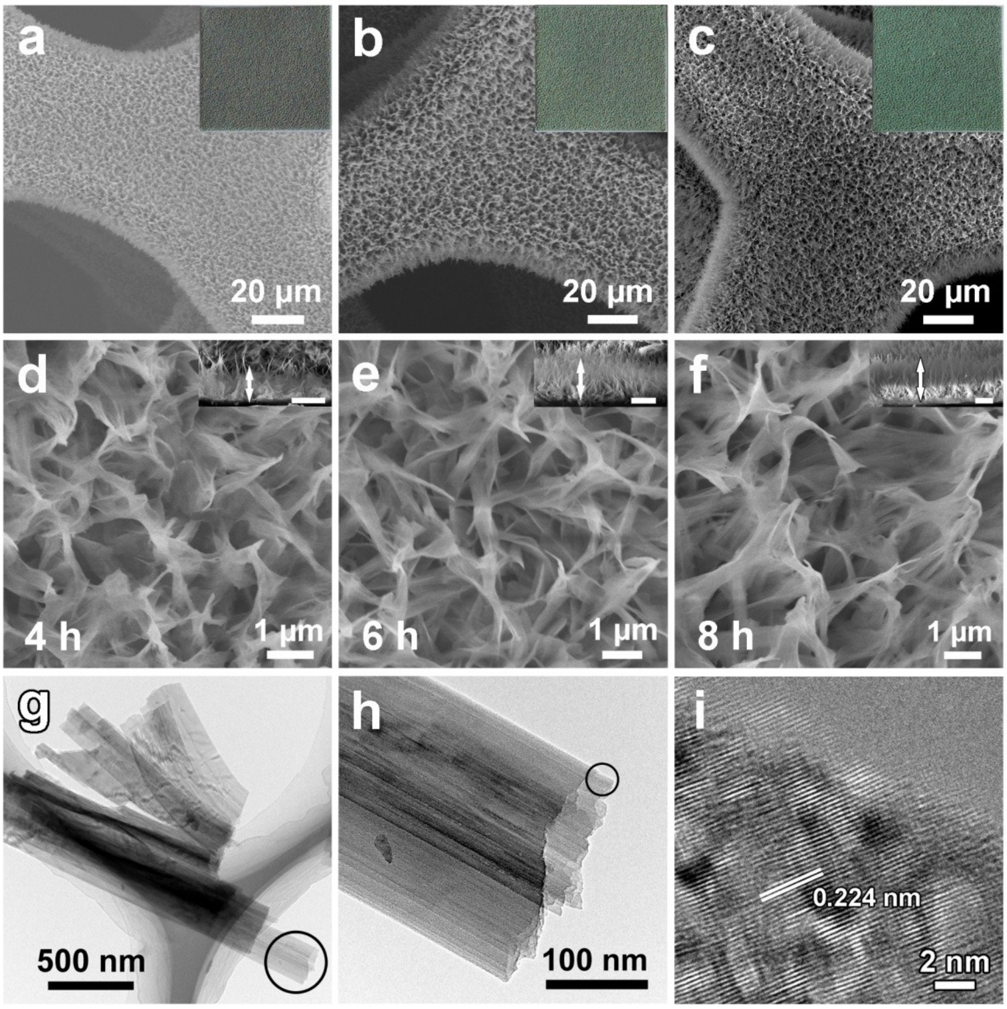

Fig. S3 Low magnified SEM images of the $Ni(SO_4)_{0.3}OH_{1.4}$ precursor with synthesis time of 4 h (a), 6 h (b) and 8 h (c). The insets show the green color of the precursors turn darker along with the prolonged reaction time. (d-f) High magnified SEM images of the precursors with belt shape. They have little difference in morphology except the length. The lengths of the precursors are shown in the insets with scale bars of 5 μm. The lengths are ~5, ~8 and ~11 μm corresponding to the reaction time of 4, 6, and 8 hrs, respectively. (g, h) TEM images of the $Ni(SO_4)_{0.3}OH_{1.4}$ precursor with synthesis time of 6 h. Fig. S3h is taken from the marked region in Fig. S3g. (i) HRTEM image corresponding to the circle in Fig. S3h. The lattice spacings of 0.22 nm are in accord with the (2 1 -2) planes of the $Ni(SO_4)_{0.3}OH_{1.4}$ in agreement with the above XRD result.

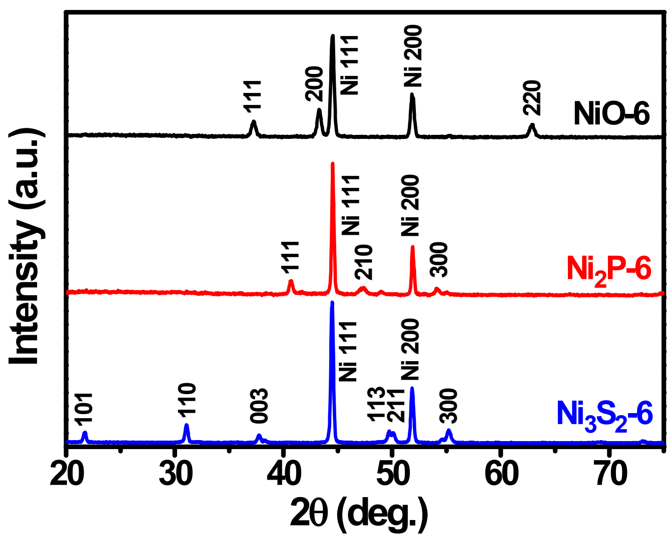

Fig. S4 XRD patterns of the NiO@NF-6, Ni_2P@NF-6 and Ni_3S_2@NFi-6. The peaks confirm the component of NiO, Ni_2P, and Ni_3S_2 in agreement with JCPDS No. 47-1049, 74-1385, and 44-1418, respectively. The strong peaks come from the Ni foam as marked in the patterns.

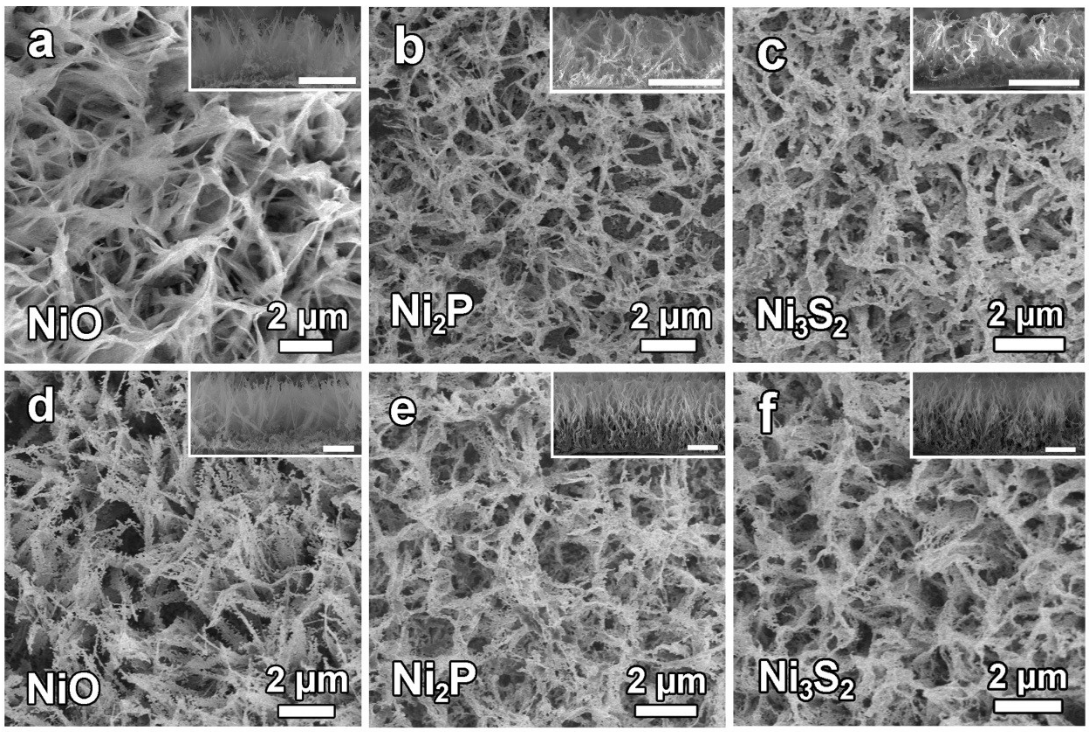

Fig. S5 (a-c) SEM images of NiO@NF-4, Ni_2P@NF-4, and Ni_3S_2@NF-4 and (d-f) SEM images of NiO@NF-8, Ni_2P@NF-8 and Ni_3S_2@NF-8 in sequence. The corresponding insets show the thickness of the samples with scale bars of 5 μm. The film thickness of NiO@NF-4, Ni_2P@NF-4 and Ni_3S_2@NF-4 were ~5 μm while the thickness of NiO@NF-8, Ni_2P@NF-8 and Ni_3S_2@NF-8 were ~11 μm, in accordance with the film thickness of their precursors.

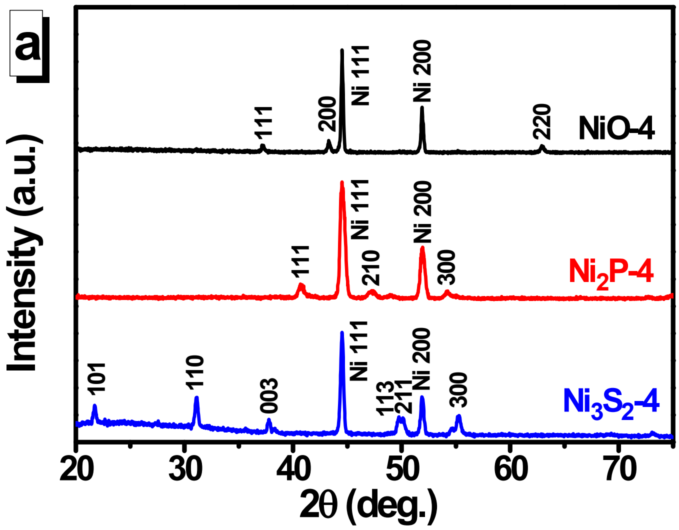

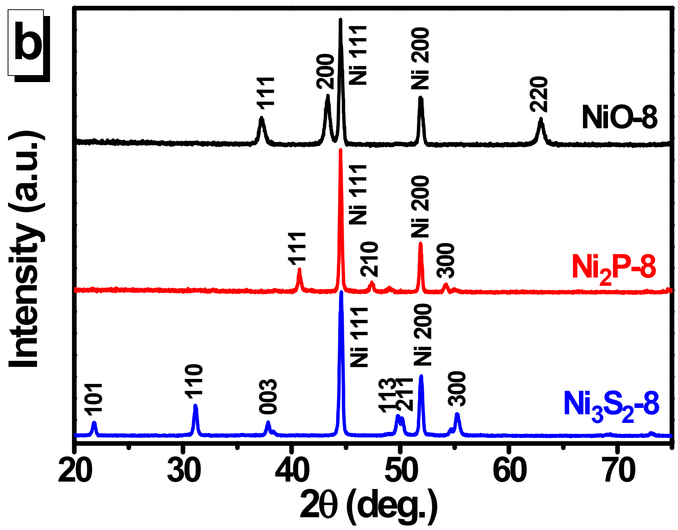

Fig. S6 (a) XRD patterns of the NiO@NF-4, the Ni_2P@NF-4, and the Ni_3S_2@NF-4. (b) XRD patterns of the NiO@NF-8, the Ni_2P@NF-8, and the Ni_3S_2@NF-8. The Ni_xM_y@NF-4 (M=O, S, P) and the Ni_xM_y@NF-8 have the same components with the Ni_xM_y@NF-6 as shown in Fig. S4.

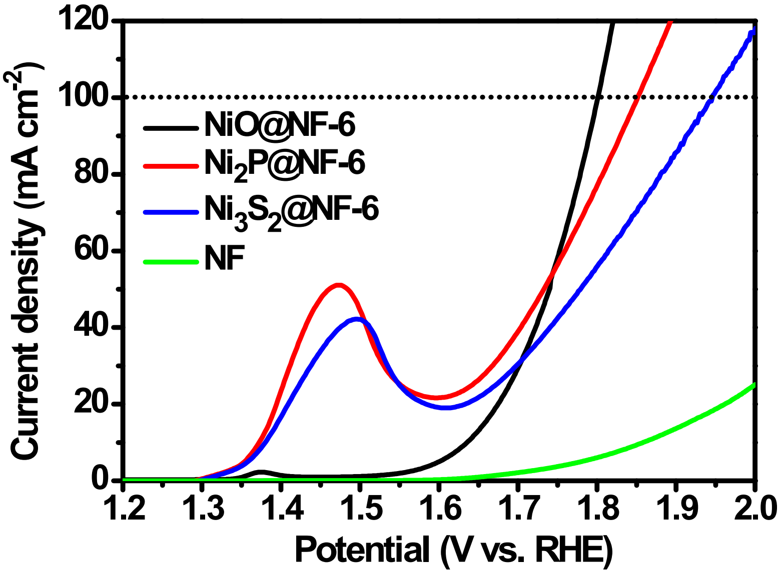

Fig. S7 LSV data of the NiO@NF-6, Ni_2P@NF-6, Ni_3S_2@NF-6 samples and the NF in 1.0 mol L^{-1} KOH aqueous solution with a scan rate of 5 mV s^{-1} for OER. The overpotential of NiO@NF-6 was 570 mV at 100 mA cm^{-2}, 55 mV and 147 mV less than that of Ni_2P@NF-6 and Ni_3S_2@NF-6. The current density of NF could not reach 30 mA cm^{-2} at the overpotential of 770 mV.

Table S1 Comparison of OER activity of the NiO@NF-6 with recently reported NiO-based catalysts.

Electrode	Electrolyte	Loading (mg cm^{-2})	η @ 10 mA cm^{-2} (mV)	Tafel slop (mV dec^{-1})	Reference
NiO@NF-6	1 M KOH	3.5	405	109	Our work
15-30 nm NiO NPs	0.1 M KOH	0.36	396	54	Nano Energy, 2015, 12, 115-122
~40 nm NiO NPs	1 M KOH	0.2	427	117	Chem. Commun., 2015, 51, 7851-7854
8-30 nm NiO NPs	0.1 M KOH	0.21	510	N.A.	Angew. Chem. Int. Ed. 2014, 53, 8508-8512
~3.8 nm NiO NPs	0.5 M KOH	0.088	325	N.A.	ACS Nano, 2015, 9, 5180-5188
$Ni_xCo_{3-x}O_4$ nanowires	1 M KOH	0.7	337	75	ACS Appl. Mater. Interfaces, 2016, 8, 3208-3214
$NiFeO_x$/carbon fibre paper	1 M NaOH	1.6	350	44	Nat. Commun. 2015, 6, 7261
Ni-Co_2-O hollow nanosponges	1 M KOH	0.2	362	64	Chem. Commun., 2015, 51, 7851-7854
Fe-nitrogen-carbon sheets/NiO	0.1 M KOH	0.24	390	76	Angew. Chem. Int. Ed. 2015, 54,10530-10534
nitrogen-doped multiwall carbon nanotubes/NiO-Ni	1 M KOH	0.21	400	80	Angew. Chem. Int. Ed. 2015, 54, 9654-9658
8-30 nm Ni_xO_y/ nitrogen-doped carbon	0.1 M KOH	0.21	410	N.A.	Angew. Chem. Int. Ed. 2014, 53, 8508-8512

Table S2 Values of Overpotentials and Tafel slopes of a series of NiO@NF, Ni_2P@NF, and Ni_3S_2@NF electrodes for OER.

Electrode	Overpotential (mV, 10 mA cm^{-2})	Overpotential (mV, 100 mA cm^{-2})	Tafel slope (mV dec^{-1})
NiO@NF-4	484	655	121
NiO@NF-6	405	570	109
NiO@NF-8	486	/	152
Ni_2P@NF-4	156	704	304
Ni_2P@NF-6	142	625	297
Ni_2P@NF-8	152	664	303
Ni_3S_2@NF-4	163	/	362
Ni_3S_2@NF-6	151	717	337
Ni_3S_2@NF-8	161	/	355
NF	620	/	223

/ could not reach 100 mA cm^{-2} in the voltage range we selected.

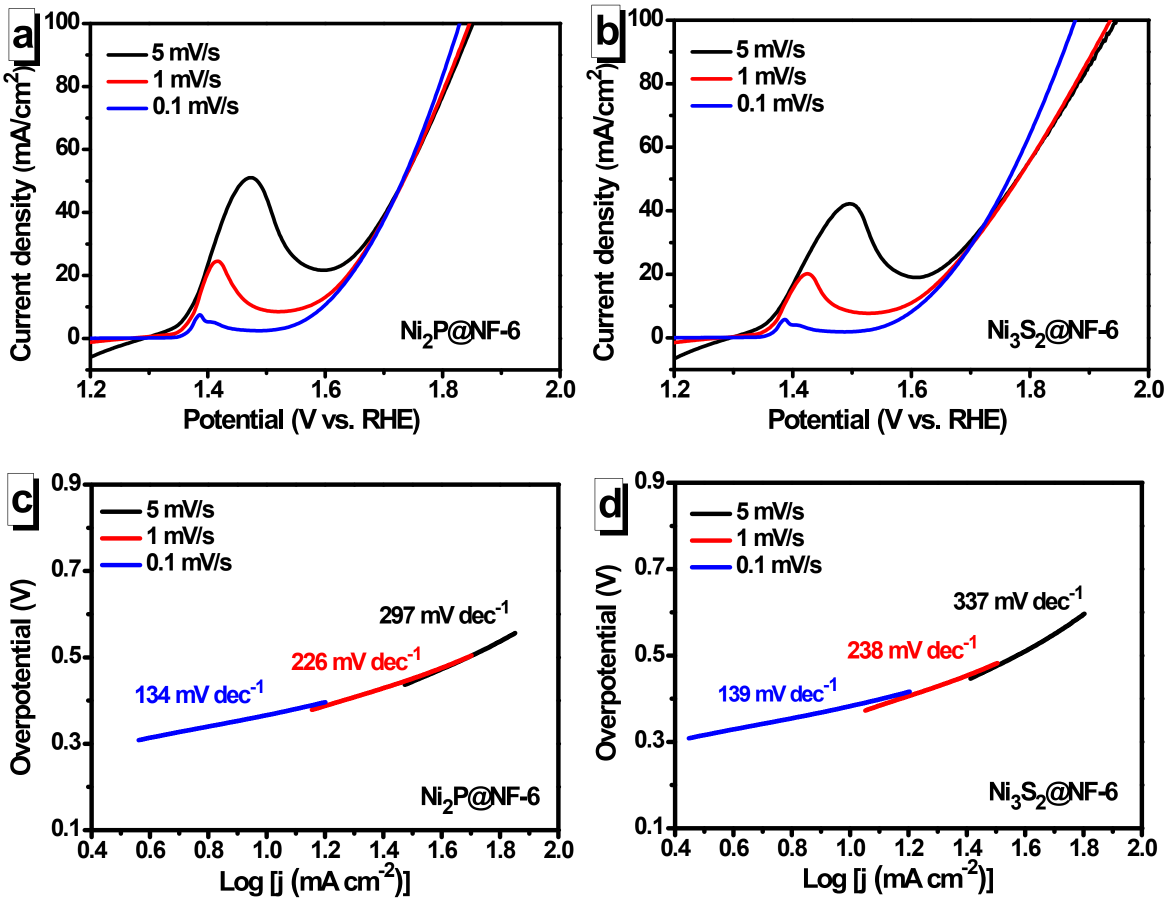

Fig. S8 LSV curves of (a) Ni_2P@NF-6 and (b) Ni_3S_2@NF-6 in 1 mol L^{-1} KOH aqueous solution with a scan rate of 5, 1 and 0.1 mV s^{-1} for OER, respectively. (c) and (d) the corresponding Tafel plots.

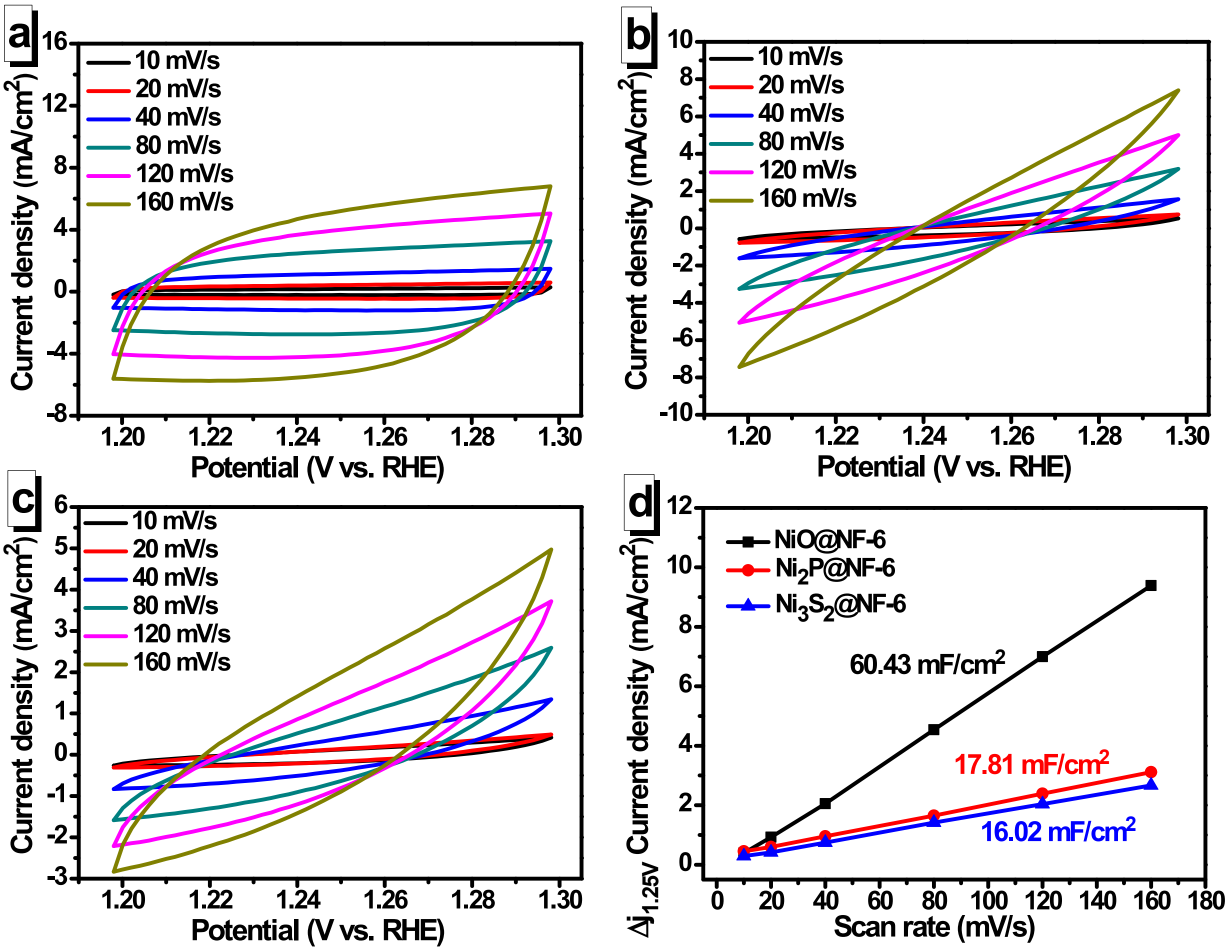

Fig. S9 Cyclic voltammograms of (a) NiO@NF-6, (b) Ni_2P@NF-6 and (c) Ni_3S_2@NF-6 obtained in 1.2-1.3 V vs. RHE region at scan rates of 10, 20, 40, 80, 120 and 160 mV s^{-1}, respectively. (d) The difference in current density (*j*) between the anodic and cathodic sweeps ($\Delta j = j_{anodic} - j_{cathodic}$) at 1.25 V vs. RHE versus scan rates for NiO@NF-6, Ni_2P@NF-6 and Ni_3S_2@NF-6. The linear slope was equivalent to twice of the double-layer capacitance (C_{dl}).

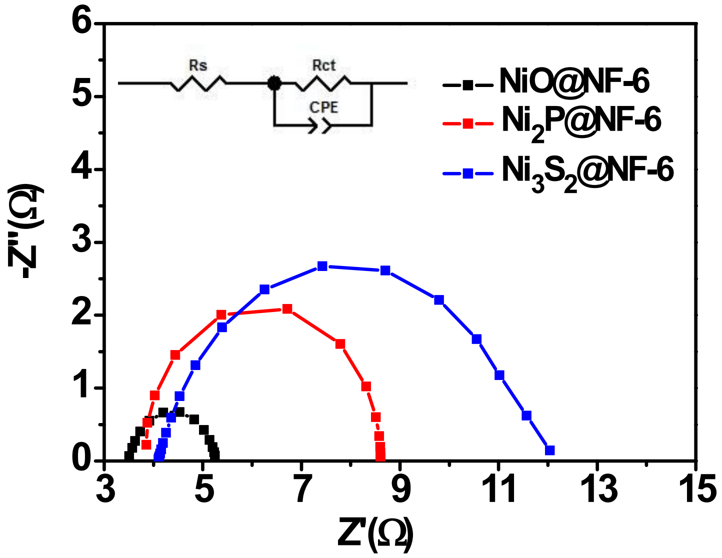

Fig. S10 Nyquist plots of the NiO@NF-6, the Ni_2P@NF-6, and the Ni_3S_2@NF-6 for OER.

The curves were obtained by AC impedance spectroscopy at around overpotential of 500 mV in 1 mol·L^{-1} KOH aqueous solution with 5 mV amplitude and frequency range from 1 Hz to 100 kHz. Inset: the corresponding equivalent circuit diagram consisting of an electrolyte resistance (R_s), a charge-transfer resistance (R_{ct}), and a constant-phase element (CPE). The R_s was obtained by the first intersection of the semicircle and the X axis while the R_{ct} equaled to the diameter of the semicircle. The R_s of the NiO@NF-6, the Ni_2P@NF-6, and the Ni_3S_2@NF-6 were 3.57, 3.88, and 4.10 Ω and the R_{ct} were 1.77, 4.37, and 7.56 Ω, respectively.

Table S3 Values of Overpotentials and Tafel slopes of a series of NiO@NF, Ni_2P@NF, and Ni_3S_2@NF electrodes for HER.

Electrode	**Overpotential (mV, 10 mA cm^{-2})**	**Tafel slope (mV dec^{-1})**
NiO@NF-4	322	263
NiO@NF-6	310	231
NiO@NF-8	331	317
Ni_2P@NF-4	114	127
Ni_2P@NF-6	99	120
Ni_2P@NF-8	121	128
Ni_3S_2@NF-4	139	161
Ni_3S_2@NF-6	114	134
Ni_3S_2@NF-8	136	163
NF	494	222

Table S4 Comparison of HER activity of the Ni_2P@NF-6 with recently reported phosphide catalysts.

Electrocatalyst	Electrolyte	Loading (mg cm^{-2})	η @ 10 mA cm^{-2} (mV)	Tafel slop (mV dec^{-1})	Reference
Ni_2P@NF-6	1 M KOH	5.6	58 (J=5) 99 (J=10) 149 (J=20)	111	Our work
Ni-P film/copper foam	1 M KOH	~5.0	98	55	J. Power Sources, 2015, 299, 342-346
Ni_5P_4 film/Ni foil	1 M KOH	13.9	159	~53	Angew. Chem. Int. Ed. 2015, 54, 12361-12365
amorphous Ni-P microsphere	1 M KOH	1.5	~170	N.A.	J. Mater. Chem. A, 2014, 2, 18593-18599
~10 nm Ni_2P NPs	1 M KOH	1.8	221	N.A.	Energy Environ. Sci., 2015, 8, 2347-2351
10-50 nm Ni_2P NPs	1 M KOH	0.38	250 (*J=20*)	100	Phys. Chem. Chem. Phys., 2014, 16, 5917-5921
17 nm Ni_2P NPs	1 M KOH	1.0	205 (*J=20*)	N.A.	J. Am. Chem. Soc. 2013, 135, 9267-9270
Ni-P nano plates	1 M KOH	0.286	350	132	Chem. Commun., 2016, 52, 1633-1636
Porous Urchin-Like Ni_2P/Ni/Ni foam	1 M KOH	77.6	98	72	ACS Catal. 2016, 6, 714-721
NiP_2 nanosheet/carbon cloth	1 M KOH	4.3	102	65	Nanoscale, 2014, 6, 13440-13445
amorphous W-doped Ni-P microsphere	1 M KOH	1.5	110 (*J=5*)	98	J. Mater. Chem. A, 2014, 2, 18593-18599
Ni-Co-P-300	1 M KOH	0.286	150	61	Chem. Commun., 2016, 52, 1633-1636

Table S5 Comparison of HER activity of the Ni_3S_2@NF-6 with recently reported sulfide catalysts.

Electrocatalyst	Electrolyte	Loanding (mg cm^{-2})	η @ 10 mA cm^{-2} (mV)	Tafel slop (mV dec^{-1})	Reference
Ni_3S_2@NF-6	1 M KOH	6.4	114 (*J=10*) 163 (*J=20*) 263 (*J=50*)	134	Our work
NiS film/NF	1 M KOH	43	158 (*J=20*)	83	Chem. Commun., 2016, 52, 1486-1489
NiS_2 nanosheets	1 M NaOH	1.2	190	80	RSC Adv., 2015, 5, 32976-32982
Ni_3S_2/NF	1 M KOH	1.6	223	N.A.	J. Am. Chem. Soc. 2015, 137, 14023-14026
$Ni_{0.33}Co_{0.67}S_2$ nanowires	1 M KOH	0.3	88	118	Adv. Energy Mater. 2015, 5, 1402031
$NiCo_2S_4$ nanowires array/ carbon cloth	1 M KOH	~4.0	263 (*J=50*)	141	Nanoscale, 2015, 7, 15122-15126

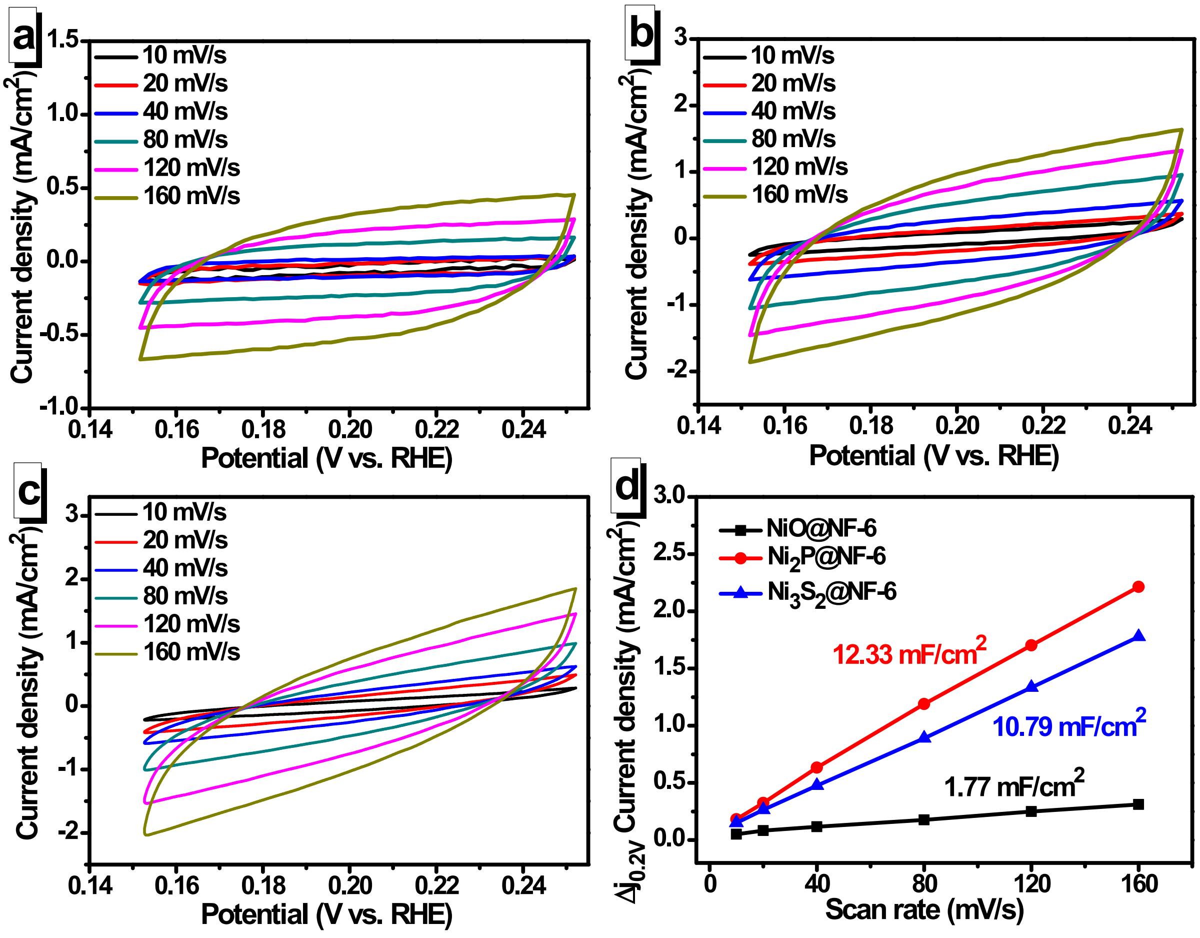

Fig. S11 Cyclic voltammograms of (a) NiO@NF-6, (b) Ni_2P@NF-6 and (c) Ni_3S_2@NF-6 obtained in 0.15-0.25 V vs. RHE region at scan rates of 10, 20, 40, 80, 120 and 160 mV s^{-1}, respectively. (d) The difference in current density (j) between the anodic and cathodic sweeps ($\Delta j = j_{anodic} - j_{cathodic}$) at 0.20 V vs. RHE versus scan rates for NiO@NF-6, Ni_2P@NF-6 and Ni_3S_2@NF-6. The linear slope is equivalent to twice of the double-layer capacitance (C_{dl}).

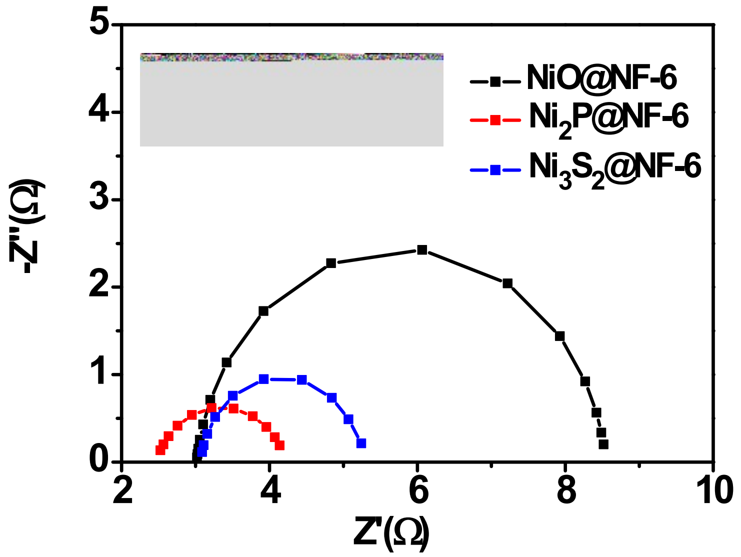

Fig. S12 Nyquist plots of the NiO@NF-6, Ni_2P@NF-6, and Ni_3S_2@NF-6 for HER.

The curves were obtained by AC impedance spectroscopy at around overpotential of 300 mV in 1 mol·L^{-1} KOH aqueous solution with 5 mV amplitude and frequency range from 1 Hz to 100 kHz. Inset: the corresponding equivalent circuit diagram consisting of a R_s, a R_{ct}, and a CPE. The R_s of the NiO@NF-6, the Ni_2P@NF-6, and the Ni_3S_2@NF-6 were 3.02, 2.53, and 3.09 Ω and the R_{ct} were 5.54, 1.76, and 2.17 Ω, respectively.

Table S6 Comparison of different Ni-based catalysts for overall water splitting with recently reported work.

Electrode pair	Electrolyte	E (V)[a]	Loading (mg cm^{-2})	Current density retention (%, h)	Reference
*NiO@NF-6 // Ni_2P@NF-6	1 M KOH	1.65	3.5 / 5.6	92, 120	Our Work
Ni_3S_2@NF-6 // Ni_2P@NF-6	1 M KOH	1.69	6.4 / 5.6	79, 30	Our Work
Ni_2P@NF-6 // Ni_2P@NF-6	1 M KOH	1.70	5.6 / 5.6	89, 30	Our Work
Ni_3S_2@NF-6 // Ni_3S_2@NF-6	1 M KOH	1.77	6.4 / 6.4	73, 30	Our Work
NiO@NF-6 // Ni_3S_2@NF-6	1 M KOH	1.76	3.5 / 6.4	83, 30	Our Work
NiO@NF-6 // NiO@NF-6	1 M KOH	1.81	3.5 / 3.5	72, 30	Our Work
NiFe LDH // NiO/Ni-CNT[b]	1 M KOH	1.50 (*J=20*)	8.0	~93, 24	Nat. Commun. 2014, 6, 4695
NiFe LDH // Ni@NiO/Cr_2O_3	1 M KOH	1.5 (*J=20*)	24	~77, 50	Angew. Chem. Int. Ed. 2015, 54, 11989-11993
$CoNi(OH)_x$ // NiN_x	1 M KOH	~1.64	0.72 / 0.75	74, 0.17 h	Adv. Energy Mater. 2016, 6, 1501661
$NiCo_2O_4$ / $Ni_{0.33}Co_{0.67}S_2$	1 M KOH	~1.72	0.3 / 0.3	~85, 20 h	Adv. Energy Mater. 2015, 5, 1402031
Ni_2P/Ni/NF // Ni_2P/Ni/NF	1 M KOH	1.49	77.6	~92, 40	ACS Catal. 2016, 6, 714-721
Ni-P/Cu foam // Ni-P/Cu foam	1 M KOH	1.68	~5.0	~72, 15	J. Power Sources, 2015, 299, 342-346
Ni-B/Ni foam // Ni-B/Ni foam	1 M KOH	1.69 (*J=15*)	12.3	~76, 10	Nanotechnology, 2016, 27, 12LT01
NiFe LDH/Ni foam // NiFe LDH/Ni foam	1 M KOH	1.70	N.A.	~73, 10	Science, 2014, 345, 1593-1596
Ni_5P_4 film Ni foil // Ni_5P_4 film Ni foil	1 M KOH	~1.70	13.9	N.A.	Angew. Chem. Int. Ed. 2015, 54, 12361-12365
Ni_3S_2/Ni foam // Ni_3S_2/Ni foam	1 M KOH	1.76 (*J=13*)	1.6	~66, 150	J. Am. Chem. Soc. 2015, 137, 14023-14026

a. J = 10 mA/cm^2; b. LDH = layered double hydroxide, CNT = carbon nanotube.
* a well matched electrode pair for overall water splitting.
All the current density retention and stability of the reported papers were tested by chronoamperometry.

Table S7 The NiO@NF-4//Ni_xM_y@NF-4 and NiO@NF-8//Ni_xM_y@NF-8 (M=O, S, and P) electrode pairs for overall water splitting.

Electrode pair	Electrolyte	E (V, J=10 mA cm^{-2})	Loading (mg cm^{-2})
NiO@NF-4 // Ni_2P@NF-4	1 M KOH	1.77	2.7 / 4.5
NiO@NF-4 // Ni_3S_2@NF-4	1 M KOH	1.79	2.7 / 5.0
NiO@NF-4 // NiO@NF-4	1 M KOH	1.99	2.7 / 2.7
NiO@NF-8 // Ni_2P@NF-8	1 M KOH	1.73	5.0 / 8.1
NiO@NF-8 // Ni_3S_2@NF-8	1 M KOH	1.80	5.0 / 8.5
NiO@NF-8 // NiO@NF-8	1 M KOH	1.97	5.0 / 5.0

Table S8 Summary of electrochemical performance using Ni_xM_y@NF-6 (M=O, S, and P) as electrodes for overall water splitting.

OER	HER	Potential (V, 10 mA cm^{-2})	Superiority of electrochemical performance
NiO@NF-6	Ni_2P@NF-6	1.65	**Overall water splitting: NiO@NF-6** // Ni_2P@NF-6 > **NiO@NF-6** // Ni_3S_2@NF-6 > **NiO@NF-6** // NiO@NF-6 **HER:** Ni_2P@NF-6 > Ni_3S_2@NF-6 > NiO@NF-6
	Ni_3S_2@NF-6	1.76	
	NiO@NF-6	1.81	
Ni_2P@NF-6	Ni_2P@NF-6	1.70	**Overall water splitting: Ni_2P@NF-6** // Ni_2P@NF-6 > **Ni_2P@NF-6** // Ni_3S_2@NF-6 > **Ni_2P@NF-6** // NiO@NF-6 **HER:** Ni_2P@NF-6 > Ni_3S_2@NF-6 > NiO@NF-6
	Ni_3S_2@NF-6	1.75	
	NiO@NF-6	1.84	
Ni_3S_2@NF-6	Ni_2P@NF-6	1.69	**Overall water splitting: Ni_3S_2@NF-6** // Ni_2P@NF-6 > **Ni_3S_2@NF-6** // Ni_3S_2@NF-6 > **Ni_3S_2@NF-6** // NiO@NF-6 **HER:** Ni_2P@NF-6 > Ni_3S_2@NF-6 > NiO@NF-6
	Ni_3S_2@NF-6	1.77	
	NiO@NF-6	1.84	
NiO@NF-6	**Ni_2P@NF-6**	1.65	**Overall water splitting:** NiO@NF-6 // **Ni_2P@NF-6** > Ni_2P@NF-6 // **Ni_2P@NF-6** ≈ Ni_3S_2@NF-6 // **Ni_2P@NF-6** **OER:** NiO@NF-6 > Ni_2P@NF-6 > Ni_3S_2@NF-6
Ni_2P@NF-6		1.70	
Ni_3S_2@NF-6		1.69	
NiO@NF-6	**Ni_3S_2@NF-6**	1.76	**Overall water splitting:** NiO@NF-6 // **Ni_3S_2@NF-6** ≈ Ni_2P@NF-6 // **Ni_3S_2@NF-6** ≈ Ni_3S_2@NF-6 // **Ni_3S_2@NF-6** **OER:** NiO@NF-6 > Ni_2P@NF-6 > Ni_3S_2@NF-6
Ni_2P@NF-6		1.75	
Ni_3S_2@NF-6		1.77	
NiO@NF-6	**NiO@NF-6**	1.81	**Overall water splitting:** NiO@NF-6 // **NiO@NF-6** > Ni_2P@NF-6 // **NiO@NF-6** ≈ Ni_3S_2@NF-6 // **NiO@NF-6** **OER:** NiO@NF-6 > Ni_2P@NF-6 > Ni_3S_2@NF-6
Ni_2P@NF-6		1.84	
Ni_3S_2@NF-6		1.84	

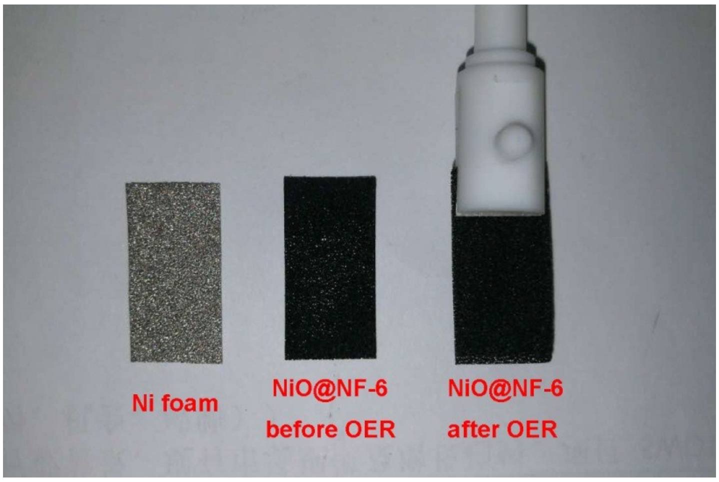

Fig. S13 The optical photo of the Ni foam, the NiO@NF-6 before and after long-term OER tests.

The Ni foams were fragile after heat treatment under high temperature in our experiments. Considering the aim of this manuscript to fabricate well-paired electrodes by choosing suitable nickel compounds, we didn’t take deep consideration before. The NiO@NF-6 could maintain the structure in our careful long-term OER test.